EFFECTS OF Cu AND Ag ON PRECIPITATION IN Al-4Zn-3Mg (wt. %).

Sally K. CARAHER, Ian J. POLMEAR and Simon P. RINGER.

Department of Materials Engineering, Monash University, Clayton 3168, Australia.

ABSTRACT Details are given of a preliminary investigation into the precipitation sequences during age hardening in a series of Al-4Zn-3Mg (wt %) alloys containing single and combined additions of 0.85 Cu and 0.5 Ag (wt. %). Hardness testing, conventional transmission electron microscopy and electron diffraction have been used to study the precipitation processes at 150 °C. The results suggest that this ageing temperature may be above the GP zone solvus for these alloys, with extensive precipitation of η'/η_2 precipitation observed on $\{111\}_\alpha$ planes. These precipitates are bound by continuous $\{111\}_\alpha$ facets. The observed crystallographic form of the precipitates has been examined in terms of lattice misfit for various structural models of η' and proposals are presented to explain the observed precipitate form and morphology.

Keywords: *precipitation, Al-Zn-Mg alloys, η' precipitation, age hardening*

1. INTRODUCTION

Alloys based on the Al-Zn-Mg (7xxx series) are of major importance as light weight structural materials because of their high response to age hardening. It is well known that the addition of Cu (e.g. ~ 1.5 wt. %) is beneficial in both increasing tensile properties and decreasing susceptibility to stress corrosion cracking [e.g. 1]. Similar effects are also observed in Al-Zn-Mg alloys containing small amounts (e.g. 0.5 wt. % or 0.1 at. %) of Ag [2]. However, questions remain concerning the effects of these two elements in the precipitation process occurring during ageing of this class of alloys.

This paper presents preliminary results of a study of the effects of single and combined additions of 1 wt. % Cu and 0.5 wt. % Ag on precipitation in a base alloy of composition Al-4Zn-3Mg (wt. %) aged at 150 °C. Special attention has been given to the crystallographic form and distribution of $\{111\}_\alpha$ precipitates in these alloys.

2. EXPERIMENTAL

The compositions of the alloys studied were as follows: Alloy 1: Al-4Zn-3Mg (wt. %), Alloy 2: Al-4Zn-3Mg-0.5Ag (wt. %), Alloy 3: Al-4Zn-3Mg-0.85Cu (wt. %) and Alloy 4: Al-4Zn-3Mg-0.5Ag-1Cu (wt. %). Alloy specimens for Vickers hardness measurements and transmission electron microscopy (TEM) were solution treated in a salt bath at 460 °C for 1h, cold water quenched and aged in oil baths at 150 °C. Specimens for TEM examination were twin-jet electropolished using standard techniques and examined in a Philips CM20 analytical TEM operating at 200 kV.

3. RESULTS AND DISCUSSION

3.1 Age Hardening Characteristics

The age hardening characteristics for the four Al-4Zn-3Mg-(Ag, Cu) (wt. %) alloys at 150 °C are presented in Fig. 1. The hardening trends indicated in Fig. 1 are in good agreement with the previous studies of age hardening in this system [2]. Rapid hardening at the early stages of ageing was noted for both of the Cu-containing alloys. This effect appears similar to that observed in recently discussed in detail for Al-Cu-Mg alloys [3].

3.2 Microstructural Evolution at 150 °C

The microstructural evolution in the Al-4Zn-3Mg-(Ag, Cu) alloys at 150 °C was studied by conventional TEM. A typical bright field (BF) TEM image, recorded near to the $<110>_\alpha$ zone axis, of the alloys in the AQ condition is provided in Fig. 2. There was little evidence of an extensive

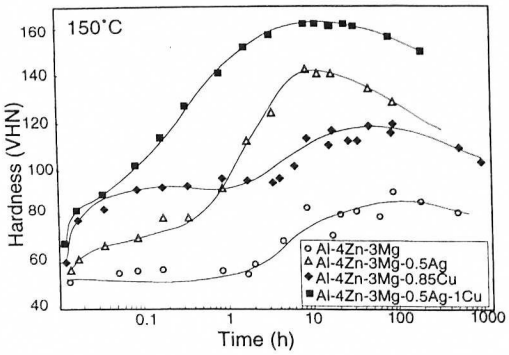

FIGURE 1. Hardness-time curves for the Al-4Zn-3Mg-(Ag, Cu) alloys aged at 150 °C.

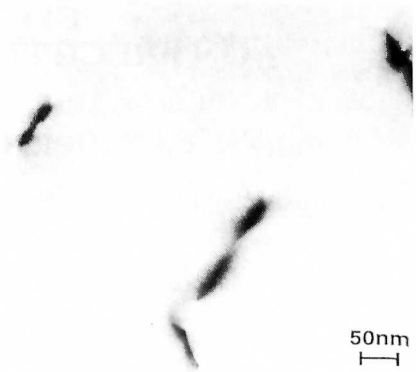

FIGURE 2. $<110>_\alpha$ BF TEM image of the AQ microstructure of alloy 1.

quenched-in defect structure in $<100>_\alpha$ or $<110>_\alpha$ BF TEM images of alloy samples in the AQ condition (Fig. 2). There was no evidence of precipitation in BF TEM images or in corresponding selected area electron diffraction (SAED) patterns. These results suggest that the high Mg concentration in the base alloy results in the capture of most of the excess vacancies from the quench leaving few vacancies free for coalescence and defect formation following the quench [4].

A sequence of $<110>_\alpha$ BF TEM images were also recorded for alloys 1-4 after ageing for 5 min, 2 h, 19.25 h and 1500 h at 150 °C and representative fields are presented in Figs. 3(a)-(d), respectively. The present study focused on the general intragranular precipitation, which was of a considerably finer scale and occurred uniformly throughout the matrix. Inspection of Fig. 3 indicates that most of this precipitation seems to have occurred on $\{111\}_\alpha$ planes.

Figure 4 is a $<110>_\alpha$ SAED pattern recorded from the Al-4Zn-3Mg-0.5Ag (wt. %) alloy in the peak hardness condition (aged 19.25h at 150 °C), Fig. 3(b). This pattern is representative of the alloys studied in that it contains diffraction effects which were common to all alloys, to a greater or lesser extent, through the various stages of ageing. The precise interpretation of the set of $<110>_\alpha$ SAED patterns recorded for all conditions examined in Fig. 3 is complicated because of the diffuse nature of the η' diffraction, which arises from the very fine precipitate sizes. This is compounded by ambiguity regarding the crystal structure of this phase, for which a number of structural models have been proposed [e.g. 5] and by the similarity in lattice parameters between η' and the equilibrium η phase ($MgZn_2$, C14, a=0.521 nm, c=0.860 nm), which is known to occur in up to 6 orientations, designated η_1 - η_6 [6]. At this stage, not all effects in the SAED patterns have been unambiguously identified and comparison of the experimental patterns and those predicted by the various structural models for η' and η phase could not account for all experimentally observed diffractions. However, the presence of the η' phase was identified on the basis of reflections present at 1/3 and 2/3 $\mathbf{g}\{220\}_\alpha$. These reflections are consistent with the structural model of η' proposed by Auld and Cousland (P6m2, a=0.496 nm, c=1.402 nm) [7] where $d_{(10.0)\eta'}=3d_{(220)\alpha}$ and $d_{(00.1)\eta'}=6d_{(111)\alpha}$. Since $(10.0)_\eta//\{110\}_\alpha$, $(00.1)_\eta//\{111\}_\alpha$, these reflections are clearly different from diffractions by the equilibrium η phase, Fig. 4. The present work has focused on the form and distribution of precipitates which occurred on $\{111\}_\alpha$ planes, which corresponds to the majority of precipitates observed in the alloy series. Where ambiguity regarding the $\{111\}_\alpha$ precipitate identity exists, the designation η'/η_2 precipitation has been used to indicate the possible presence of η' or the equilibrium η_2 precipitate, oriented $(10.0)_{\eta 2}//\{110\}_\alpha$ and $(00.1)_{\eta 2}//\{111\}_\alpha$. Comments on the specific effects of alloying with Cu and Ag on the nature and dispersion of these precipitates follow below.

Alloy 1: Al-4Zn-3Mg (wt. %) Alloy

The $<110>_\alpha$ BF TEM images provided in Fig. 3(a) reveal no evidence of precipitation after ageing for 5 min. at 150 °C. This ageing time is well within the hardness incubation period (Fig. 1) though Fig. 3(a) also reveals little or no uniform precipitation even after ageing for 2 h. At peak hardness (96 h at 150 °C, Fig. 3(a)) η'/η_2 precipitation was observed in the form of blocky platelets with $\{111\}_\alpha$ habit planes. The overaged condition (1500 h. at 150 °C, Fig. 3(a)) was characterised by a slightly coarser distribution of η'/η_2 precipitation.

FIGURE 3. (a)Al-4Zn-3Mg (b)Al-4Zn-3Mg-0.5Ag

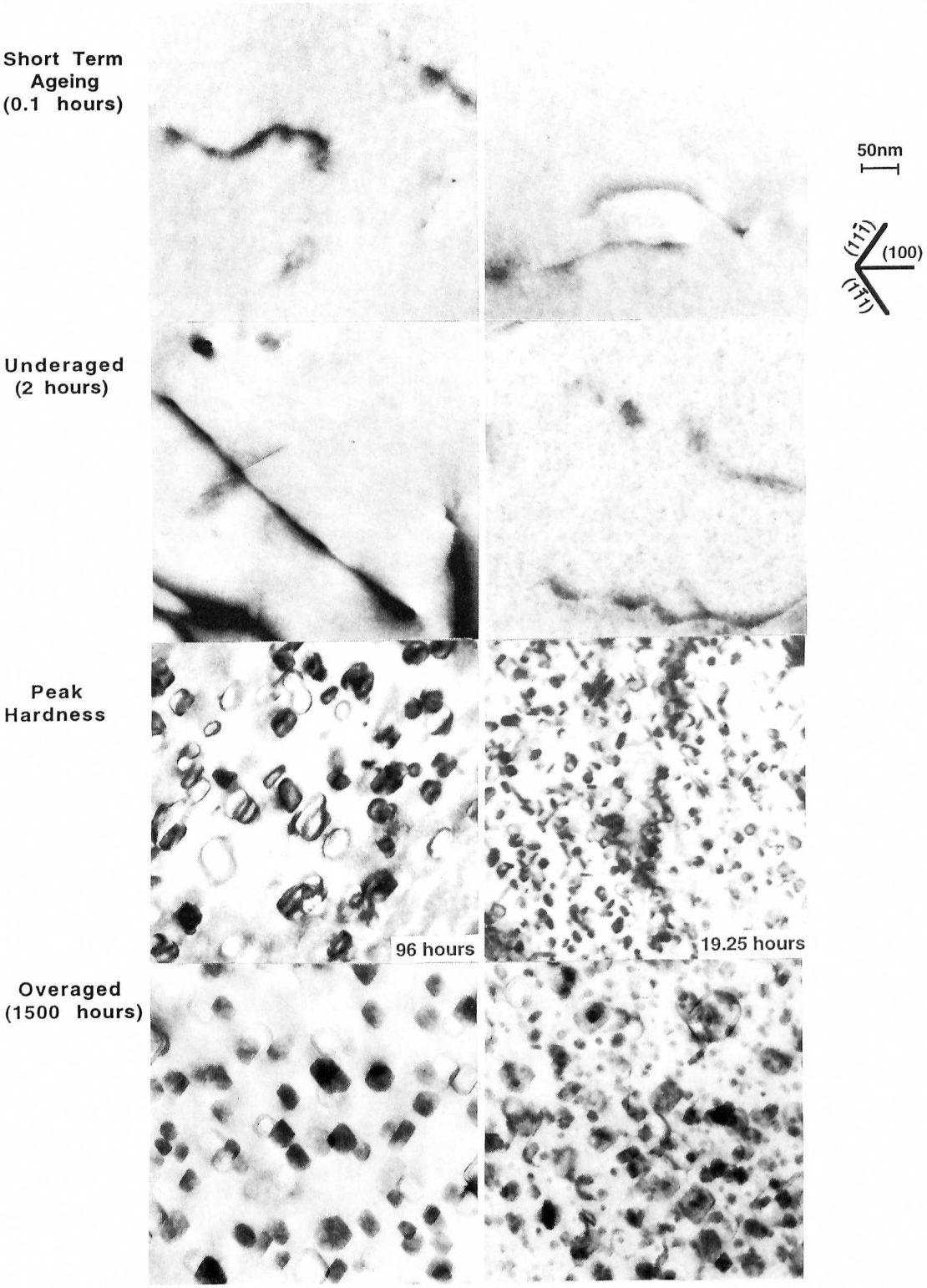

FIGURE 3 (cont.) (c) Al-4Zn-3Mg-1Cu (d) Al-4Zn-3Mg-0.5Ag-1Cu

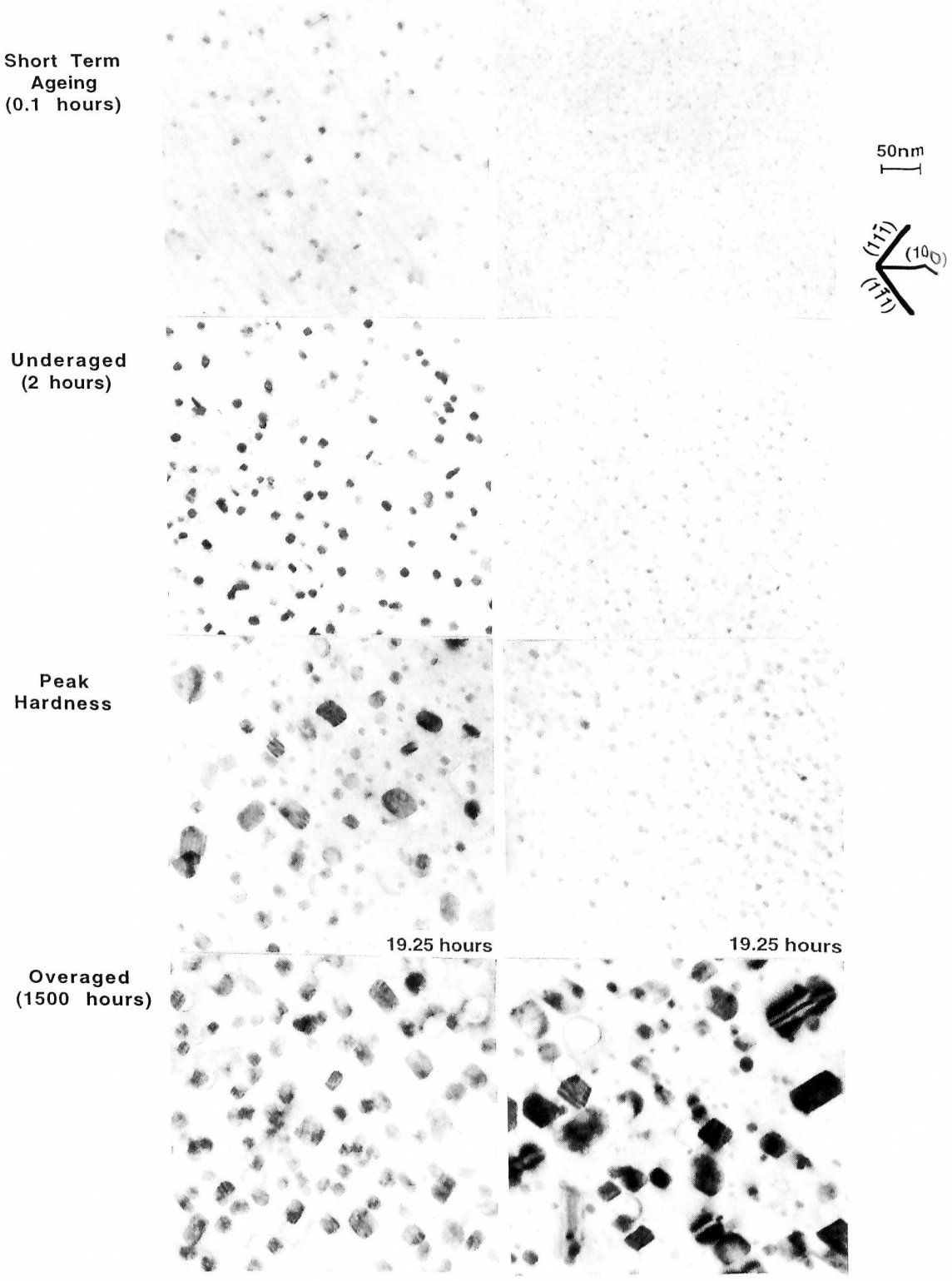

Alloy 2: Al-4Zn-3Mg-0.5Ag (wt. %) Alloy

Figure 3(b) reveals that a fine and uniform distribution of precipitates has developed after 5 min. Further precipitation was apparent after 2 h ageing (Fig. 3(b)) and the intragranular precipitates exhibited clear $\{111\}_\alpha$ habit planes. The size, trace and SAED effects at 1/3 and 2/3 $\mathbf{g}\{220\}_\alpha$ identified these precipitates as the η' phase and they were considered to be the coarser products of growth of the precipitates observed after 5 min. At peak hardness (aged 19.25 h at 150 °C, Fig. 3(b)), at least two distinct precipitates were observed. The first appeared identical in shape and trace, but smaller in size to the η'/η precipitates observed on $\{111\}_\alpha$ planes in the base alloy, while the second type exhibited facets parallel to the $\{001\}_\alpha$ planes and were likely to be η_1 precipitates, viz: $(10.0)_{\eta 1}//\{001\}_\alpha$ and $(00.1)_{\eta 1}//\{110\}_\alpha$. Overageing was associated with the gradual coarsening of the η'/η precipitates.

Alloy 3: Al-4Zn-3Mg-0.85Cu (wt. %) Alloy

Figure 3(c) indicates that the precipitation process is at least bimodal in the Cu containing alloy. A relatively coarse dispersion of the η'/η_2 precipitates was observed on the $\{111\}_\alpha$ planes as early as 5 min and these develop into coarser precipitates having $\{111\}_\alpha$ facets during subsequent ageing. It is considered unlikely that these features are responsible for the rapid early hardening. Another precipitation process involves the formation of extremely fine-scale precipitates observed only after 2 h ageing (Fig. 3(c)). These images contained evidence that these precipitates also possessed a $\{111\}_\alpha$ trace, suggestive that they are highly refined η', though the detailed identity of these features remains unclear. Nevertheless, most if not all precipitates observed at peak hardness and in overaged microstructures were $\{111\}_\alpha$ faceted η'/η_2 precipitates (Fig. 3(c)).

Alloy 4: Al-4Zn-3Mg-0.5Ag-1Cu (wt. %) Alloy

Figure 3(d) reveals that the quinary Ag-Cu-containing alloy possessed the finest microstructures of the present series, which is consistent with the age hardening observations (Fig. 1). Platelets with ~ 5 nm diameter were observed on $\{111\}_\alpha$ planes after 5 min. ageing and these were coarser and more clearly resolved following 2 h ageing. Gradual coarsening of the η'/η_2 platelets follows with further ageing.

It is noteworthy that perfectly spherical GP zones were not observed in the present alloys examined following ageing at 150 °C. Furthermore, at peak hardness and in overaged microstructures, observations of other orientations of η were made (η_{1-9}) although a detailed characterisation of the effects of Cu and Ag on these orientations is not provided here.

3.3 Form and Structure of $\{111\}_\alpha$ Precipitates

A common feature of all $\{111\}_\alpha$ precipitates observed in the four alloys was the presence of continuous faceting on $\{111\}_\alpha$ planes when viewed edge-on in $<110>_\alpha$ BF TEM images. This observation held for both the finest η' precipitates, as well as coarser η'/η_2 platelets. This seems to be in contrast to the Ω, T_1 and X' precipitates which also occur on the $\{111\}_\alpha$ planes in Al-Cu-Mg-(Ag, Li) based alloys [3, 8] and are sometimes compared, crystallographically, to η'. Those precipitates are generally bound by a semi-coherent rim or edge parallel to the $\{112\}_\alpha$ planes, normal to their habit plane. The crystallographic form of η' phase observed here was considered in terms of lattice misfit across the precipitate and matrix for the various structural models of the η' crystal [see e.g. 5]. The result for the η' structure proposed by Auld and Cousland [7] is shown in Fig. 5. Here, a sketch of the basic Bravais lattice of the η' unit cell (Fig. 5(a)) and the correspondence of the η'/α lattices in the $(10.0)_{\eta'}//\{110\}_\alpha$ projection where $(10.0)_{\eta'}//\{110\}_\alpha$ and $(00.1)_{\eta'}//\{111\}_\alpha$ (Fig. 5(b)) are both provided. The shaded region in Fig. 5(b) represents the outline of the observed crystal form, whilst the dotted line outlines the unit cell of η'. The $\{111\}_\alpha$ facets are parallel to $(00.1)_{\eta'}$ and $(\bar{1}2.2)_{\eta'}$. For the assumed crystal structure, the d-spacings for these planes are 1.402 nm and 0.2338 nm, respectively, which in turn correspond to $6d_{\{111\}\alpha}$ and $d_{\{111\}\alpha}$. Therefore, there is a near zero misfit across these planes, which is in contrast to the 1.24 % misfit which would accumulate for growth across the $\{112\}_\alpha//(\bar{1}2.0)_{\eta'}$ planes. Moreover, this was the best matching found for all of the proposed structures for η' phase [5]. This result may be significant given the difficulty in obtaining clear diffraction data uniquely from the η' phase and is regarded as tacit support for the crystal structure proposed by Auld and Cousland or for something very close to it. This observation may partially explain why there is such limited growth of the η' phase along or across the habit plane, since the misfits are negligible for both of these facets with the result that there may be little driving

force for the nucleation of new ledges and further growth. Finally, the observed aspect ratio is considerably smaller (approximately 1-3) than the other $\{111\}_\alpha$ precipitates which occur in Al-Cu-Mg-(Ag, Li) based alloys (approximately 20-100). This is consistent with the equivalent and negligible misfit across all of the $\{111\}_\alpha$ facets, which form the η'/α interface. Further work is in progress to clarify the precise crystal structure of the η' phase and to unambiguously distinguish the diffraction effects of GP zones, η' and η precipitates in these alloys.

4. CONCLUSIONS

1. The AQ microstructures of the base Al-4Zn-3Mg (wt. %) alloy and those containing Cu and/or Ag, possess a low defect density, suggesting that most of the excess vacancies are retained in a super-saturated solid solution (SSSS) after quenching.
2. The precipitation process was dominated by the formation of $\{111\}_\alpha$ phases, with the peak hardness and overaged microstructures rather similar in all alloys. This suggests that the addition of Cu and Ag seem to influence mostly the kinetics of precipitation rather than introduce new metastable precipitates, when aged at 150 °C. The present results show a significant refinement of the η'/η_2 precipitates associated with Cu and Ag additions. Following this preliminary study, the dominant precipitation processes seem to include:
   Alloy 1: SSSS $\rightarrow \eta'/\eta_2 \rightarrow \eta_2$ $(+\eta_{1\text{-}9})$ Alloy 2: SSSS $\rightarrow \eta' \rightarrow \eta'/\eta_2 + \eta_l \rightarrow \eta_2$ $(+\eta_{1\text{-}9})$
   Alloy 3: SSSS $\rightarrow \eta'/\eta_2 \rightarrow \eta_2$ $(+\eta_{1\text{-}9})$ Alloy 4: SSSS $\rightarrow \eta' \rightarrow \eta'/\eta_2 \rightarrow \eta_2$ $(+\eta_{1\text{-}9})$
3. Conventional TEM did not reveal the cause of the rapid early hardening observed in the two Cu-containing alloys. It is possible that this effect arises from the formation of solute clusters.
4. Examination of the η' precipitates revealed that they possess continuous $\{111\}_\alpha$ faceting. This crystallographic form has been shown to offer tacit support to the structure for η' proposed by Auld and Cousland, or something very close to it, since this structure accumulates an equivalent and negligible misfit both across and within the habit plane. This observation was also linked to the low aspect ratio observed for the η' precipitate phase, since the near perfect lattice registry would seem to restrict the nucleation of new growth ledges.

REFERENCES

[1] H.Y. Hunsicker, Proc. Rosenhain Centenary Conf., Roy. Soc., London, (1976), 245.
[2] I. J. Polmear, J. Inst. Metals, 87(1960), 51.
[3] S.P. Ringer, T. Sakurai and I.J. Polmear, Acta Metall. Mater., 45(1997), 3731.
[4] C. Panseri and T. Federighi, Acta Metall., 11(1963), 575.
[5] A. Yamamoto, K. Minami, U. Ishihara and H. Tsubakino, Mater. Trans. JIM, 39(1998), 69.
[6] J. Gjønnes and C.J. Simensen, Acta Metall., 18(1970), 881.
[7] J. H. Auld and S. Mck. Cousland, J. Austrln. Inst. Met., 19(1974), 194.
[8] B.C. Muddle, S.P. Ringer and I.J. Polmear, Trans. Mat. Res. Soc. Japan, 19B(1994), 999.

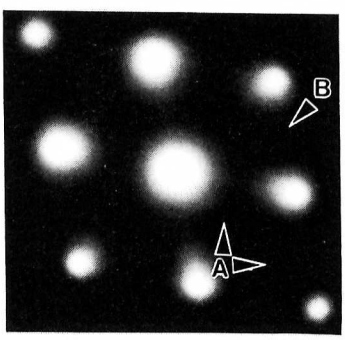

FIGURE 4. $<110>_\alpha$ SAED pattern from alloy 2 after ageing to peak hardness. Diffractions effects from η' (A) and η (B) phases are labelled.

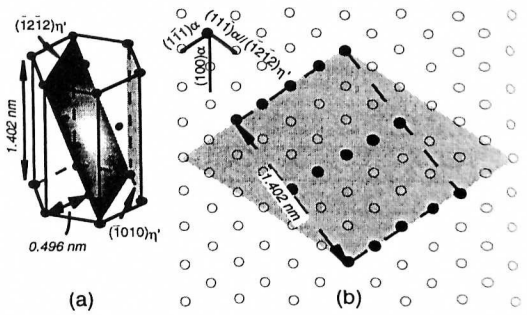

FIGURE 5. (a) Bravais lattice of the Auld and Cousland structural model for η' [7], (b) lattice correspondence viewed along $<110>_\alpha$. Shaded is the observed crystal form of the η' precipitates whilst the dotted outline traces the side-view of the η' unit cell.